Exploring Malus' Law and Determining Brewster's Angle for a Glass Slide with a Laser-Polarizer Setup

Joonwoo Noh(260973555), Keonwoo Kim(260914383)

McGill University Department of Physics

February 23, 2025

Abstract

Using a partially polarized laser beam directed through a polarizer, we verified Malus' law by showing that the transmitted intensity follows a $\cos^2(\theta)$ pattern. We then investigated the Brewster's angle of a glass slide in two distinct ways. First, by measuring transmitted intensity over a range of incidence angles, we found Brewster's angle of $57.921 \pm 0.007°$, corresponding to an index of refraction of $n_{glass} = 1.5954 \pm 0.0004$. Second, by measuring the normal-incidence transmission and applying a direct Fresnel relation, we obtained Brewster's angle of $56.717 \pm 0.002°$ and $n_{glass} = 1.5233 \pm 0.0001$, which aligns more closely with standard glass values. Finally, shining the laser at Brewster's angle allowed us to identify the absolute polarization orientation of the laser beam.

Contents

1 Introduction

Light, an electromagnetic wave, consists of an electric field $\mathbf{E}$ and a magnetic field $\mathbf{B}$. These two fields are perpendicular to each other, and also perpendicular to the direction of wave propagation $\hat{\mathbf{k}}$. When the light is unpolarized, the components of $\mathbf{E}$ and corresponding components of $\mathbf{B}$ can point in all directions perpendicular to $\hat{\mathbf{k}}$. However, passing the light through a polarizer removes the field components perpendicular to the polarizer's transmission axis, leaving the electric and magnetic fields oriented in a specific direction.

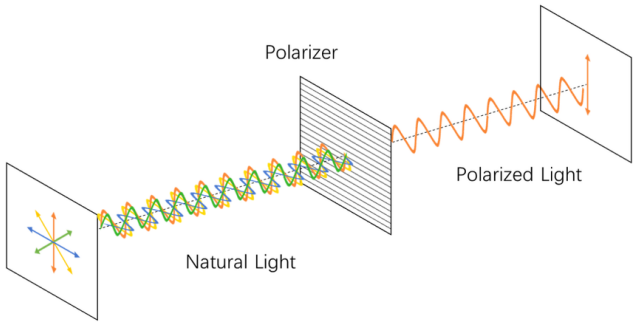

Figure 1: Configuration illustrating how unpolarized light becomes polarized. Only the electric field components parallel to the polarizer's transmission axis remain. (Image adapted from [1].)

1.1 Malus' Law

Since the field components perpendicular to the polarizer's transmission axis are blocked, the transmitted light intensity diminishes according to Malus' law:

$$I = I_0 \cos^2 \theta, \tag{1}$$

where I is the intensity of light after passing through the polarizer, I_0 is the initial intensity of the polarized light before the polarizer, and θ is the angle between the polarizer's transmission axis and the incident light's polarization direction [1].

1.2 Brewster's Angle

When light illuminates a glass surface, some of it is reflected while the remainder is refracted into the glass. In the special case where the reflected and refracted beams are orthogonal, the reflected beam becomes fully polarized, meaning its electric field **E** is parallel to the interface. This angle of incidence is called Brewster's angle. At Brewster's angle, the reflected intensity is minimized because it contains only the parallel (p-polarized) component; at other angles, reflection includes both parallel and perpendicular components (i.e., remains unpolarized) and thus exhibits higher intensity. From Brewster's angle θ_B, one can find the refractive index of the medium:

$$\tan \theta_B = \frac{n_2}{n_1}, \tag{2}$$

where n_1 is the refractive index of the initial medium and n_2 is that of the transmission medium [2].

To check whether a measured θ_B is consistent, one may also use the ratio of the reflected to the incident intensity,

$$R = \left(\frac{n_1 - n_2}{n_1 + n_2}\right)^2, \tag{3}$$

which provides an alternative route to determining n_2 [2].

1.3 Fresnel Equation

A more detailed Fresnel analysis of reflection and transmission at a single interface gives the p-polarized reflection coefficient $R_p(\theta_i)$ as:

$$R_p(\theta_i) = \left(\frac{n_1 \cos\theta_t - n_2 \cos\theta_i}{n_1 \cos\theta_t + n_2 \cos\theta_i}\right)^2 = \left(\frac{n_1\sqrt{1 - \left(\frac{n_1}{n_2}\sin\theta_i\right)^2} - n_2\cos\theta_i}{n_1\sqrt{1 - \left(\frac{n_1}{n_2}\sin\theta_i\right)^2} + n_2\cos\theta_i}\right)^2, \tag{4}$$

where θ_i and θ_t are the angles of incidence and transmission, respectively [3]. Assuming negligible absorption or scattering in the glass, energy conservation implies

$$T_p(\theta) = 1 - R_p(\theta), \tag{5}$$

so $T_p(\theta)$ describes the fraction of p-polarized light transmitted at incidence angle θ [2].

In the work below, we measured the light transmitted through the glass at various incidence angles and fit our data to the simplified Fresnel form in Eq. (5). This procedure identifies the angle where reflection is minimized (or transmission peaks), yielding the Brewster angle and the refractive index n_2. Concretely, the photodiode recorded output over a range of angles, and we performed a nonlinear fit to compare those intensities with the theoretical $T_p(\theta)$ curve.

2 Materials and Methods

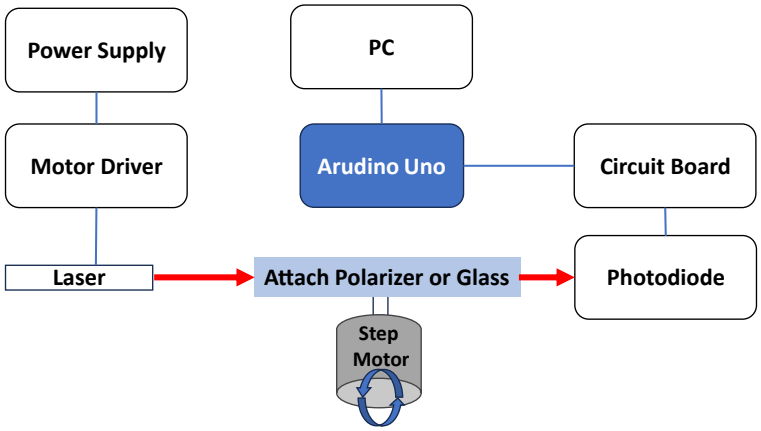

Figure 2: Experimental apparatus. A laser illuminates a rotating element (polarizer or glass slide) mounted on a stepper motor, while a photodiode detects the transmitted intensity.

All experiments were conducted using a laser, a rotating element (either a polarizer or a glass slide) driven by a stepper motor, and a photodiode circuit for measuring transmitted light. The laser served as the light source, with either a polarizer or a glass slide attached to the motor downstream. Arduino, fitted with a stepper motor shield, controlled the motor's incremental rotations and read the photodiode's analog output, which is proportional to the detected light intensity.

For data acquisition, Arduino stepped the motor at a set increment, recorded the photodiode reading, and sent these data to a computer for analysis. When studying Malus' law, the polarizer was rotated from 0 to 360° in small increments to map how the transmitted intensity varies with the polarizer angle. For determining Brewster's angle, the glass slide

was rotated similarly, typically from normal incidence (0°) up to angles of about 70–80°, while monitoring the photodiode output to identify minima or maxima in reflection or transmission. We excluded data from the range of 80° to 90° because, at these angles, the glass became parallel to the laser, resulting in inaccurate measurements. Furthermore, we also verified that the stepper motor didn't miss any steps by moving it forward by 400 steps (one full rotation) and then moving it backward by 400 steps. We confirmed that it returned precisely to the initial position.

3 Part 1: Malus' Law and Laser Polarization

3.1 Results

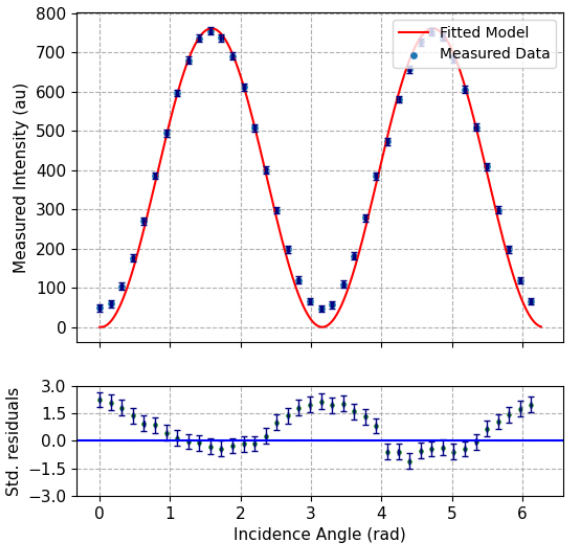

Figure 3: The x-axis represents the stepper motor's angle from the arbitrary initial reference, measured in radians, while the y-axis shows the light intensity in arbitrary units (au). The residual plot is standardized for clarity. The graph displays 40 scattered data points with error bars, highlighting the symmetry around the angle π, which reflects the polarizer's symmetry relative to its transmission axis. The fitted curve follows the equation $I = 761\cos^2(\theta + 0.494\pi)$.

With a polarizer mounted on the stepper motor, we recorded how the photodiode's analog voltage changed at each motor step, revealing how the transmitted light intensity depends on

the polarizer angle. Because we did not know the absolute angular position of the polarizer, we defined an arbitrary zero point. In Fig. (3), we plotted the intensity data against the corresponding stepper motor angles. For clearer visualization, only 40 out of the 400 collected data points are displayed, though the full dataset was used for analysis. Using all 400 data points, we performed a curve fitting to determine if the results align with Malus' law Eq. (1).

3.2 Discussion

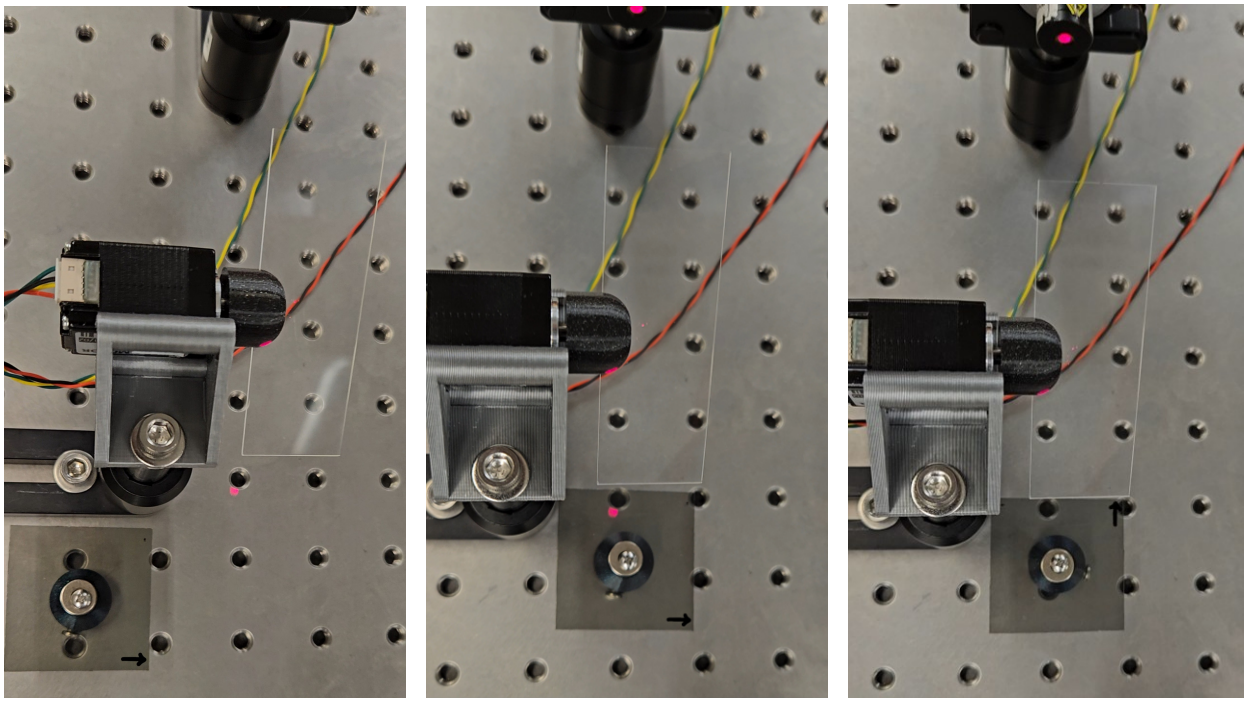

(a) (b) (c)

Figure 4: The polarizer's orientation is indicated by an arrow on its surface. (a) The laser was directed at Brewster's angle through the glass, with the reflected light hitting the metal surface. (b) At this orientation, the reflected light appeared at its brightest. (c) After rotating the polarizer 90° counterclockwise from the previous position, the reflected light completely disappeared.

To minimize random errors and enhance precision, we rotated the polarizer through 400 steps and repeated this process 10 times (i.e., 10 complete revolutions). The data presented in Fig. (3) corresponds to the first rotation. The fitted curve follows the equation $I = 761\cos^2(\theta + 0.494\pi)$. Since the polarizer was rotated from an arbitrary initial angle, a phase shift of 0.494π is present.

To evaluate the fit quality, we calculated the reduced chi-squared value, χ^2_ν, for each of the 10 rotations and averaged the results, yielding $\chi^2_{\nu,\text{avg}} = 0.835 \pm 0.003$. The degrees of freedom were set to 398, as two parameters—amplitude and phase—were estimated from 400 data points. Given that $\chi^2_{\nu,\text{avg}}$ is close to 1, the measured data aligns well with Malus' law.

In Fig. (3), each data point includes horizontal and vertical error bars, though they are too small to be visually apparent. The circuit voltage deviated slightly from 5V due to noise from nearby equipment. To estimate the voltage uncertainty (and thus the intensity uncertainty), we used an oscilloscope to measure the circuit's maximum and minimum voltages. The observed fluctuation was 0.12V; however, we considered half of this value, 0.06V, as the uncertainty, representing the average deviation. This translates to an uncertainty of 9.11 au. For the horizontal error, we assigned an uncertainty of 1 step, corresponding to 0.016 radians.

Expanding the experiment, we adjusted the glass slide to Brewster's angle determined in section (4), ensuring the incident angle matched Brewster's angle. At this angle, the reflected light from the glass is perfectly polarized. By observing the reflected light through the polarizer at different orientations, we determined the absolute polarization direction of the laser. As shown in Fig. (4)(c), the reflected light completely disappeared at a specific polarizer orientation, confirming perfect polarization. This result was cross-verified by testing at angles other than Brewster's angle, where the reflected light dimmed but never fully vanished regardless of the polarizer's orientation. In Fig. (4)(b), the reflected light appeared brightest when the electric field was entirely parallel to the transmission axis of the polarizer, indicating no perpendicular component. Consequently, we conclude that the laser's absolute polarization is parallel to the polarizer's marked arrow.

4 Part 2: Brewster's Angle and Light Transmission

4.1 Results

We investigated the Brewster's angle of a glass slide using two different strategies. First, we performed a nonlinear fit of the Fresnel equation (5). In total, 4000 data points were

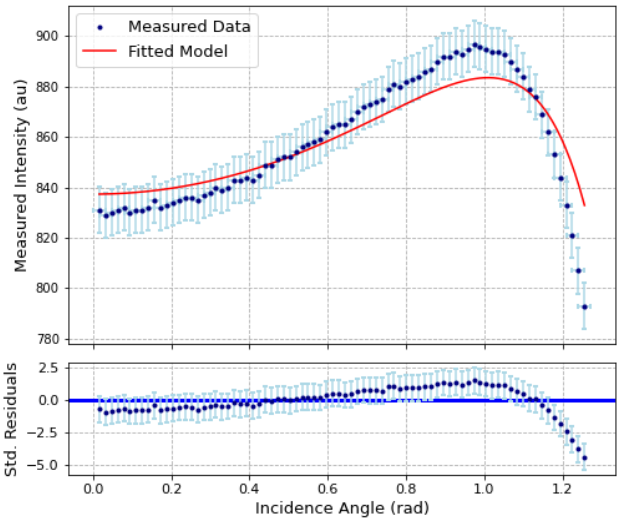

Figure 5: Angles are measured relative to the beam's perpendicular incidence (in radians). The y-axis is the detected intensity (in arbitrary units), and the lower panel shows standardized residuals. The dataset (the first 80 points from the first cycle) is overlaid with a fit corresponding to Eq. (5)

collected over 10 cycles, each cycle contributing 80 steps spanning from 0 to about 1.25 rad (72°). Fitting this dataset yielded a mean Brewster's angle of 1.0109 ± 0.0001 rad (i.e., $57.921 \pm 0.007°$) and a mean refractive index $n_2 = 1.5954 \pm 0.0004$, with a mean reduced chi-squared of $\chi^2_{\nu,\text{avg}} = 1.253 \pm 0.007$. These statistics suggest our data and error estimates are generally consistent with the expected model, though some systematic effects may remain.

In the second approach, we measured the transmitted light at normal incidence, I_{normal}, through the glass slide and compared it to I_{max}, the maximum intensity without the slide. Defining transmission coefficient $T_0 = I_{\text{normal}}/I_{\text{max}}$, we obtained an average T_0 of 900.6 ± 0.3 across ten trials. Converting each T_0 to reflectance via $R_0 = 1 - T_0$, we applied Eq. (3) to solve for n_2, finding an average of 1.5233 ± 0.0001. Plugging these n_2 values into Eq. (2) gave a mean Brewster's angle of 0.98990 ± 0.00004 rad, which is equal to $56.717 \pm 0.002°$.

4.2 Discussion

Results from the first approach—fitting the measured transmission curves to the T_p model in Eq. (5)—gave Brewster's angle slightly higher than the typical $n_2 \approx 1.52$ literature value for standard plate glass [4], along with a reduced chi-squared value, slightly higher than

1, indicating the fit was not entirely ideal. Such discrepancies likely stem from systematic factors, including alignment offsets—for instance, mechanical play or backlash in the motor assembly, small tilt angles in the glass mount, or a slight mismatch between the laser beam axis and the motor's rotation axis—that cause the true incidence angle to differ from the nominal step-based angle. Minor inaccuracies in the stepper motor's angle calibration further compound these deviations, producing the observed discrepancies from the ideal Fresnel model. These effects can lead to higher residuals and reduced chi-squared values.

By contrast, the second method—measuring normal-incidence transmission relative to the maximum intensity with no glass—proved more direct and yielded Brewster's angle closer to the literature value. Because this method relies on the two intensity measurements, it is less prone to systematic errors. It does not require rotating the glass over many angles or fitting multiple parameters, making it simpler to implement and less sensitive to subtle misalignments. Consequently, the second approach appears more robust for determining Brewster's angle under these experimental conditions.

5 Conclusion

By shining a laser through a rotating polarizer, we measured how the transmitted intensity varies with the polarizer's orientation. From these data, we verified Malus' law, obtaining a mean reduced chi-squared of $\chi^2_{\nu,\text{avg}} = 0.835 \pm 0.003$, which is sufficiently close to 1 to indicate a good fit. We also determined the laser's absolute polarization direction by setting the incidence angle on the glass plate to the Brewster angle, where the reflected beam completely vanishes.

In assessing the Brewster angle of the glass slide, we employed two methods. The first, involving a fit of the $T_p(\theta)$ model Eq. (5) over a range of angles, exposed certain systematic issues and produced a value slightly higher than the standard literature index. In contrast, the simpler technique—comparing normal-incidence transmission to the maximum intensity without the slide—yielded a Brewster angle closer to well-known glass parameters, while minimizing alignment and modeling complexities. Despite minor discrepancies, both approaches confirm that the slide's refractive index is broadly consistent with typical optical glass.

References

[1] D. Li, X. Wang, W. Zhang *et al.*, "A polarized structured light method for the 3d measurement of high-reflective surfaces," *ResearchGate*, 2023, page 4. 1

[2] D. J. Griffiths, *Introduction to Electrodynamics*, 5th ed. Cambridge University Press, 2024, page 412, 416. 2, 3

[3] RP Photonics, "Fresnel equations," n.d., accessed: 2025-02-22. [Online]. Available: https://www.rp-photonics.com/fresnel_equations.html 2

[4] LibreTexts, "Typical results for refractive index determination of glass," n.d., accessed: 2025-02-23. [Online]. Available: https://chem.libretexts.org/Ancillary_Materials/Laboratory_Experiments/Wet_Lab_Experiments/Analytical_Chemistry_Labs/ASDL_Labware/Forensic_Science_Laboratory/Glass/Typical_Results_for_Refractive_Index_Determination_of_Glass 7